JOURNAL OF SOLID STATE CHEMISTRY 50, 70–78 (1983)

Differential Scanning Coulometric Titrometry: Application to the System Co–Ni–O at 1000°C

EIJI TAKAYAMA

National Institute for Research in Inorganic Materials, Sakura-mura, Niihari-gun, Ibaraki-ken 305, Japan

Received February 23, 1983; in revised form June 24, 1983

A novel technique involving solid state coulometric titration using stabilized zirconia electrolytes is presented. The method is termed differential scanning coulometric titrometry (DSCT). It is useful for the phase equilibrium studies of multicomponent oxide systems. In the DSCT, two independent and isostructural galvanic cells are used. One is a sample cell in which a sample is charged, while the other is a reference cell without a sample. Under the condition that oxygen activities in both cells are equal to each other, coulometric titration is carried out continuously in both cells. The difference between the titration currents provided to both cells corresponds to the amount of oxygen which is allowed to react with a sample per unit time. If the difference is recorded with respect to the oxygen activity, it starts to deviate from a base line when the sample starts to be oxidized or reduced. This method was successfully applied to the system Co–Ni–O at 1000°C. The phase diagram of the system and related thermodynamic data were obtained.

Introduction

Solid state coulometric titration, using stabilized zirconia electrolytes, has been applied mainly to nonstoichiometric oxide systems such as FeO (*1–6*), CuO (*7*), and NiO (*8*). Recently, Weppner *et al.* emphasized that coulometric titration possesses several advantages compared to the quenching method or thermogravimetry in establishing phase diagrams for multicomponent systems which contain variable valence elements, and in determining related thermodynamic data (*9, 10*). Using this method, they determined the phase diagram of the system Cu–Ge–O (*10*).

However, this technique has the following problems in application to phase equilibrium studies.

(a) Since electronic (hole) conductivity in a stabilized zirconia electrolyte is significant in magnitude at temperatures over 900°C, oxygen permeation through the electrolyte cannot be neglected at these temperatures (*6*). To minimize inaccuracies caused by the oxygen permeation, serious limitations are introduced into the galvanic cell design or experimental procedures, including experimental temperature (*6*).

(b) Coulometric titration is essentially a sequence of equilibria. A certain amount of oxygen is electrochemically carried to or removed from a sample. After the system reaches the equilibrium state, the cell voltage is measured to obtain the resulting oxygen activity of the sample. This procedure must be repeated to cover the desired range of oxygen concentration in the sample. It

0022-4596/83 $3.00

takes a long time, therefore, to establish a whole phase diagram for a multicomponent system.

(c) Oxygen at reduced pressure or a mixture of O_2 with an inert gas is usually used as atmosphere around a sample in the conventional technique. At low oxygen fugacities, the oxygen transport rate to or from the sample becomes quite small in these systems (*11*). Therefore, much time is spent until the cell voltage arrives at a new equilibrium value after a titration step. It is, no doubt, more suitable to use a "buffering" gas system such as CO_2–CO or CO_2–H_2 (*11*) for an experiment at low oxygen fugacities. However, if a buffering gas system is employed, the charge passed through the electrolyte is not directly related to the change in the oxygen concentration of a sample. For instance, if the CO_2–CO system is used, a part of the charge is concerned with the following gas reaction:

$$CO_2 \rightleftarrows CO + \tfrac{1}{2}O_2 \qquad [I]$$

It is, therefore, difficult to use the buffering gas system in the usual manner.

In the present paper, a dynamical coulometric titration method is offered which can overcome these problems. Analogous to differential scanning calorimetry, this technique is termed differential scanning coulometric titrometry (DSCT).

In the DSCT, two isostructural and independent galvanic cells are employed. One is a sample cell in which a sample is charged, while the other is a reference cell without a sample. Under the condition that oxygen activities in both cells are equal to each other, coulometric titration is carried out continuously in both cells. The difference between the titration current of the sample and the reference cell corresponds to the change of oxygen concentration in a sample. This technique was successfully applied to the system Co–Ni–O at 1000°C. The phase diagram of the system and the related thermodynamic data were obtained.

The Principle of DSCT

The construction of the galvanic cells used in the present study is as follows:

$$\underset{\mathbf{I}}{O_2\ (1\ \text{atm})},\ \underset{\mathbf{II}}{\text{Pt/CSZ/Pt}},\ \underset{\mathbf{III}}{CO_2\text{–}CO}\ \underset{\mathbf{III}}{(\text{sample})},\ \underset{\mathbf{IV}}{\text{Pt/CSZ/Pt}},\ \underset{\mathbf{V}}{\text{air}}.$$

Here, CSZ and Pt represent the calcia stabilized zirconia electrolyte and the platinum electrode, respectively. Since coulometric titration is carried out continuously in DSCT, the cell has separate potential and current electrodes. A part of the cell (**I, II, III**) works as an oxygen probe to measure oxygen activity in the compartment **III**, relative to the reference gas (O_2, 1 atm). The other part (**III, IV, V**) works as an oxygen pump for coulometric titration. Oxygen ions are carried across the electrolyte **IV** by connecting an electric source between electrode **III** and **V**.

In the DSCT, a pair of galvanic cells having the same shape is employed. One is the sample cell in whose compartment **III** a sample is charged, while the other is a reference cell. Each compartment **III** is filled with a buffering gas having an appropriate pressure (we used the CO_2–CO system in the present work). Oxygen pumps of the two cells are operated by controlling titration currents, so that oxygen activities in the compartments of two cells might change linearly with time, under the condition that they are equal to each other. To maintain this condition (of oxygen activity equality in the both cells), the amount of oxygen the sample absorbs from, or provides to, compartment **III** must be compensated by a corresponding variation in the differential titration currents provided to the oxygen pump of the sample and the reference cells.

As described in the previous section, we

must in many cases consider oxygen permeation through the electrolyte. The following equation is valid, for the sample cell, relating the titration current I_s, the number of moles of oxygen which permeate through the electrolytes into the compartment **III** per unit time $\dot{P}_s$, the number of moles of oxygen which react with a sample per unit time $\dot{m}_{O_2}$ (sample), and the number of moles of oxygen concerned with the buffering gas reaction (refer to the chemical reaction [I]) $\dot{m}_{O_2}$ (gas):

$$\left(\frac{1}{4F}\right) I_s = \dot{m}_{O_2}\,(\text{sample}) + \dot{m}_{O_2}\,(\text{gas}) - \dot{P}_s. \quad (1)$$

Here, F is the Faraday constant. Similarly, the following equation between I_r, P_r, and $\dot{m}_{O_2}$ (gas) is valid for the reference cell:

$$\left(\frac{1}{4F}\right) I_r = \dot{m}_{O_2}\,(\text{gas}) - \dot{P}_r. \quad (2)$$

It must be noted that $\dot{m}_{O_2}$ (gas) in this equation is equal to that in Eq. (1), if the following conditions are satisfied: the initial pressures of buffering gas are equal in the sample and the reference cell; the equality of oxygen activities in both cells is maintained; the volume of the sample is negligibly small compared to that of the cell.

$\dot{P}_s$ and $\dot{P}_r$ in Eqs. (1) and (2) can be expressed as follows:

$$\left(\frac{1}{4F}\right) I_{s,p} = -\dot{P}_s \quad (3)$$

$$\left(\frac{1}{4F}\right) I_{r,p} = -\dot{P}_r \quad (4)$$

Here, $I_{s,p}$ and $I_{r,p}$ mean the current which is required to cancel the oxygen permeation in the sample and the reference cell, respectively.

Under the conditions specified, by subtracting Eq. (2) from Eq. (1) using Eqs. (3) and (4),

$$\left(\frac{1}{4F}\right)(\Delta I - \Delta I_p) = \dot{m}_{O_2}\,(\text{sample}) \quad (5)$$

$$\Delta I = I_s - I_r$$

$$\Delta I_p = I_{s,p} - I_{r,p}.$$

The total amount of oxygen (M_{O_2}) which is absorbed by or removed from a sample can be evaluated from the time integral of Eq. (5):

$$\left(\frac{1}{4F}\right) \int(\Delta I - \Delta I_p)dt = M_{O_2}. \quad (6)$$

This equation shows that the change of oxygen concentration in a sample is given by the time integral of ΔI from a certain base line which corresponds to ΔI_p. ΔI_p vanishes only when CSZ tubes of the sample and the reference cell have strictly the same characteristics for oxygen permeation. Practically, ΔI_p is not equal to zero owing to differences in the electrolyte materials. However, this problem can be settled by selecting an appropriate base line when integration is performed.

On the other hand, the emf of the oxygen probe of the sample cell (E_s) is represented as follows according to the Nernst equation:

$$E_s = -(RT/4F)\ \ln [P_{O_2}\,(\text{compartment III})/P_{O_2}\,(\text{ref})]$$

where P_{O_2} is oxygen fugacity and R and T have their usual meaning. A similar equation is valid for E_r of the reference cell. In the present study, the reference oxygen pressure, P_{O_2} (ref), is one atm. In the DSCT, the condition $E_s = E_r$ must always be maintained.

If ΔI is recorded with respect to E_s, ΔI starts to deviate from a base line when the sample starts to be oxidized or reduced. The emf at this point corresponds to the equilibrium value.

Instrument

Two galvanic cells having the same shape were employed. The cell construction is schematically shown in Fig. 1. Each cell consists of two CSZ tubes (Nippon Kagaku Togyo Co. Zr-11). The outer tube (300 × 25 × 20 mm) works as an oxygen pump, and

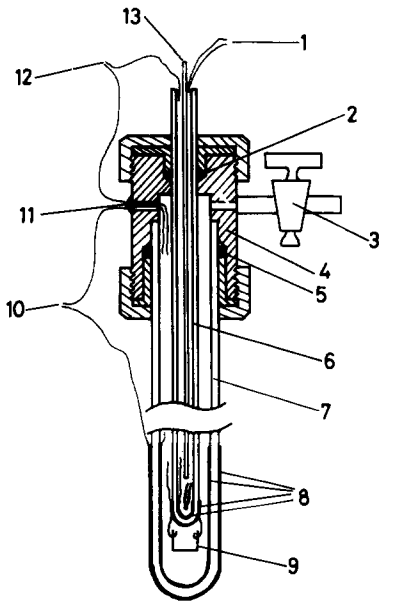

FIG. 1. Schematic diagram of a galvanic cell. 1, Pt–Pt 13% Rh thermocouple; 2, O-ring; 3, needle valve; 4, brass vessel; 5, O-ring; 6, inner CSZ tube; 7, outer CSZ tube; 8, platinum electrode; 9, alumina crucible; 10, platinum lead wire (to dc power supply); 11, epoxy seal; 12, platinum lead wire (to digital voltmeter); 13, O_2 gas inlet.

the inner tube (300 × 10 × 7 mm) works as the oxygen probe. The space between the two tubes corresponds to compartment **III**. The buffering gas can be introduced into the compartment through a needle valve which is connected to a vacuum system. To change a sample, the outer or the inner tube can be attached to or removed from a brass vessel by O-ring systems. There were no mechanical leaks at room temperature. Both cells were placed in a vertical-type furnace which had two Kanthal-wire wound heating pipes. Each heating zone was controlled independently by temperature controllers within ± 1°C.

The electrical circuit is shown in Fig. 2. Programmable dc voltage supplies (Takeda Riken Co. TR6141) were employed as electrical sources for titration. Currents passed through both oxygen pumps were measured from potential drops between standard registers connected in series to the pumps. The emf's and potential drops were measured on digital voltmeters (Datel Intersil, Inc. M4100D) which had been calibrated within ± 0.2 mv on a potentiometer (Yokogawa Electric Works, Ltd. type 2722).

Control of the system and acquisition of data were carried out on a microcomputer system (Cromemco CO. Z-2 system). A so-called PID control (proportional, integral, and derivative control) was adopted in a controlling program in order to change E_s and E_r linearly with time under the condition $E_s = E_r$. The microcomputer changed the voltage of the two dc power supplies according to the following equations:

$$V_s = -K_1(E_s - E_d) - K_2\int(E_s - E_d)dt - K_3 dE_s/dt \quad (7)$$

$$V_r = -K_1(E_r - E_d) - K_2\int(E_r - E_d)dt - K_3 dE_r/dt. \quad (8)$$

Here, V_s and V_r are voltages of the power supplies connected to the sample and the reference cell, respectively, while E_d is the desired value of emf which changes linearly with time. The three constants K_1, K_2, and K_3 were determined empirically.

Blank Test

Before this method was applied to an oxide system, a blank test was performed.

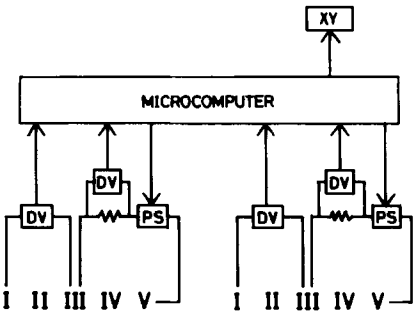

FIG. 2. Electrical circuit. DV, digital voltmeter; PS, dc power supply; XY, XY plotter. The Roman numerals denote electrodes shown in the text.

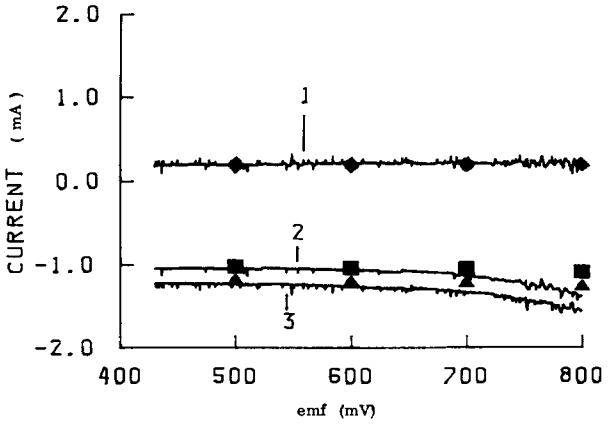

FIG. 3. The results of the blank test. 1, ΔI curve; 2, I_s curve; 3, I_r curve; ■, $I_{s,p}$; ▲, $I_{r,p}$; ◆, ΔI_p.

The sample cell (without a sample) and the reference cell were set in the furnace then heated slowly to 1000°C. Compartment **III** of each cell was evacuated and CO_2 gas was introduced. Initial pressures of CO_2 gas in both cells were equal to each other (about 150 mm Hg). First, the system was scanned to the reducing side, then scanned to the reversed side until it returned to the starting state. The scanning speed (change of rate of emf) was 5 mV/hr. In Fig. 3, the results of the reducing titration are shown. The titration current of the sample cell (I_s), that of the reference cell (I_r), and the difference of two currents (ΔI) are drawn relative to emf E_s. Current which moves oxygen into compartment III is defined as positive and emf is given with respect to a reference oxygen pressure of 1 atm. From Eq. (5), when a sample is not charged in the sample cell, the following equation is valid:

$$\Delta I = \Delta I_p. \qquad (9)$$

The ΔI curve in Fig. 3 therefore corresponds to the difference between the oxygen permeation rates for the two cells.

On the other hand, by fixing E_d in the controlling program (refer to Eqs. (7) and (8)), the titration currents required to maintain a certain oxygen activity in both cells were determined. They are $I_{s,p}$ and $I_{r,p}$ in Eqs. (3) and (4). Together with $I_{s,p}$ and $I_{r,p}$, the values of ΔI_p ($=I_{s,p} - I_{r,p}$) are shown in Fig. 3. They are situated on the ΔI curve indicating that Eq. (9) is valid. Since the galvanic cells used in the present work were very large (effective permeation area was estimated at about 80 cm^2 for each cell), $I_{s,p}$ and $I_{r,p}$ were in the milliampere range, while the difference between them is less than 0.2 mA.

Application to the Co–Ni–O System

To establish the capability of DSCT, it was applied to a rather simple system, Co–Ni–O, at 1000°C. Since an alloy phase (Co, Ni), as well as an oxide phase (Co, Ni)O, is observed in the system Co–Ni–O at 1000°C, it can be considered that the system consists of quasi-binary phases (*12*). The chemical reaction which occurs in the titration experiment is the following:

$$Co_xNi_{1-x}O \rightleftarrows [(Co, Ni) + (Co, Ni)O] \rightleftarrows Co_xNi_{1-x} + \tfrac{1}{2}O_2.$$

Oxidation or reduction proceeds via the two phase region of (Co, Ni)O and (Co, Ni).

CoO (99.9%) and NiO (99.9%) were used as starting materials. They were calcined at 1100°C for 2 days, then mixed to desired ratios in an agate mortar with ethyl alcohol.

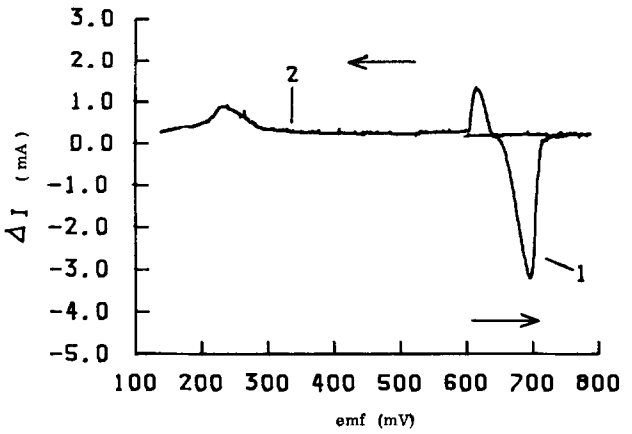

FIG. 4. ΔI curve for the reaction NiO $\rightleftarrows$ Ni + $\frac{1}{2}O_2$. 1, reduction curve; 2, oxidation curve.

The mixture thus obtained was allowed to react at 1200°C in a platinum crucible for 1 day to obtain a solid solution $Co_{1-x}Ni_xO$. It was thoroughly ground in an agate mortar, then identified by means of powder X-ray diffraction. The diffraction peaks of the solid solution were almost as sharp as those of CoO and NiO, indicating homogeneity of the solid solution. Six samples ($Co_{1-x}Ni_xO$, x = 0, 0.2, 0.4, 0.6, 0.8, 1.0) were examined.

About 30 mg of sample was placed in the sample cell. The volume of the sample was negligibly small with respect to that of the cell. The instrument was scanned first to the reducing side in the range of emf from 600 to 850 mV. After the sample was fully reduced, it was kept in a reducing atmosphere for about 12 hr to obtain a homogeneous alloy; then titration to the oxidizing side was performed for the alloy in the range of emf from 850 to 100 mV. The scanning speed was 5 mV/hr for all experiments and initial pressure of CO_2 gas was about 150 mmHg.

Pure NiO was examined first. Figure 4 shows the ΔI curve for the reaction

$$NiO \rightleftarrows Ni + \tfrac{1}{2}O_2. \qquad [II]$$

In the reducing curve, ΔI starts to deviate from the base line at emf = 646 mV, while it starts to deviate at emf = 643 mV in the oxidation curve. The average of these values (645 mV) can be regarded as the equilibrium emf of the chemical reaction [II]. In a dynamical method like that presented in this paper, it is not generally true that a detectable transformation between metal and oxide will occur exactly when the local oxygen pressure has the value corresponding to the metal/oxide equilibrium. Instead, it depends on reaction rate and kinetic conditions (*13*). However, hysteresis in the oxidation–reduction cycle was, as mentioned above, very small in the case of binary system Ni–O or Co–O.

The oxidation curve of nickel metal has two peaks, near emf = 600 and 200 mV. As shown in Eq. (5), the magnitude of deviation of ΔI from the base line corresponds to the reaction rate of oxidation or reduction. It can be seen from Fig. 4 that oxidation scarcely occurred between the two peaks of the oxidation curve. This phenomenon can be explained qualitatively as follows. At the first step of oxidation, nickel oxide is formed over nickel metal, so that further oxidation is prevented. The second step of oxidation becomes possible when the oxygen fugacity becomes much higher than that corresponding to the metal/oxide equilibrium. The shape of the ΔI curve gives

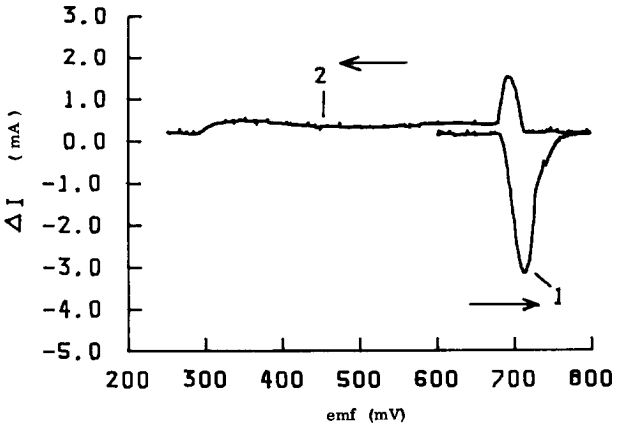

FIG. 5. ΔI curve for the reaction $Co_{0.6}Ni_{0.4}O \rightleftarrows$ [(Co, Ni) + (Co, Ni)O] $\rightleftarrows Co_{0.6}Ni_{0.4} + \frac{1}{2}O_2$. 1, reduction curve; 2, oxidation curve.

some information about the mechanism of oxidation or reduction. This may be an interesting application of DSCT.

In Fig. 5, ΔI curves are shown for the reaction

$$Co_{0.6}Ni_{0.4}O \rightleftarrows [(Co, Ni) + (Co, Ni)O] \rightleftarrows Co_{0.6}Ni_{0.4} + \tfrac{1}{2}O_2.$$

In this case, oxidation or reduction proceeds via a two phase region of (Co, Ni) and (Co, Ni)O. Therefore the emf at which the reduction of the oxide starts does not coincide with the emf at which the oxidation of the alloy starts. The oxidation curve does not consist of one strong peak like that observed with nickel metal.

All DSCT curves obtained in the present work are shown in Fig. 6, in the range of emf from 600 to 850 mV (only a part is shown for an oxidation curve). From the values of emf at which the oxidation or reduction curve starts to deviate from the base line, phase relations of the system Co–Ni–O were obtained as shown in Fig. 7. As

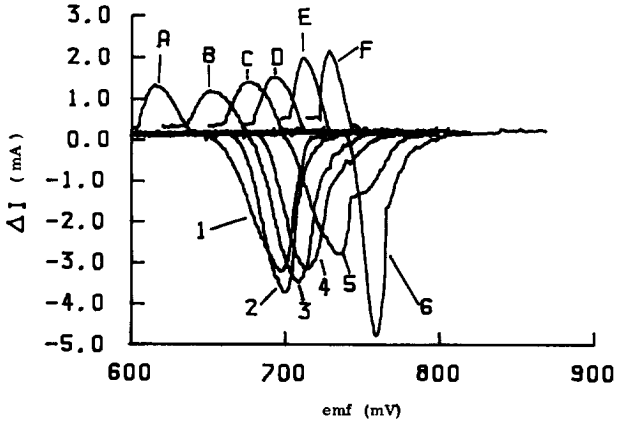

FIG. 6. ΔI curve for the reaction $Co_{1-x}Ni_xO \rightleftarrows$ [(Co, Ni) + (Co, Ni)O] $\rightleftarrows Co_{1-x}Ni_x + \frac{1}{2}O_2$. 1, 2, 3, 4, 5, and 6, reduction curves for x = 0, 0.2, 0.4, 0.6, 0.8, 1.0, respectively; A, B, C, D, E, and F, oxidation curves for x = 0, 0.2, 0.4, 0.6, 0.8, 1.0, respectively.

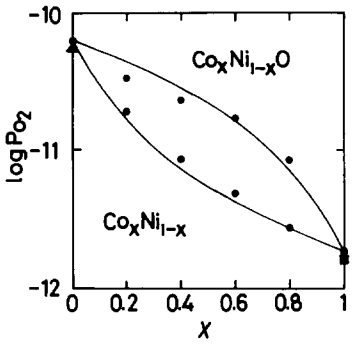

FIG. 7. Phase diagram of the system Co–Ni–O at 1000°C. ●, the present work; ▲, after Ref. (*14*); ■, after Ref. (*15*). Line is the boundary calculated based on the assumption of the ideal solutions.

to the systems Ni–O and Co–O, the equilibrium oxygen activities reported previously (*14, 15*) are also shown. They are in agreement with the data obtained in the present study within 6 mV.

If both the oxide and alloy phases can be regarded as ideal solutions, phase relations of the system Co–Ni–O can be calculated from oxygen fugacities corresponding to CoO/Co, and NiO/Ni equilibrium (*12*). The relations calculated using present results for the binary systems Co–O and Ni–O are shown in Fig. 7. Deviations from an ideal behavior are present, particularly along the oxide curve in the region $0 < x < 0.5$. Moore and White have found in a study of phase equilibrium in the system NiO–CoO–O_2 that (Co, Ni)O solutions are not strictly ideal (*16*). Nonideality of (Co, Ni)O solutions may affect the present results.

As described previously, the total amount of oxygen which reacts with a sample can be evaluated by the time integral of ΔI from a certain base line. On the other hand, it can also be calculated from the initial weight of the starting oxide. For the oxidation curve, integration is difficult because the curve is very broad. The integrated value for an oxidation curve is strongly dependent on the base line adopted. Moreover, it seems that oxidation of an alloy did not progress instantaneously due to an oxide cover over it. A reduction curve of an oxide was, therefore, used for time integration.

A base line was obtained by averaging ΔI values of a reduction curve except for a part of reduction peak. Numerical integration was performed using the data stored in the microcomputer system. Table I compares the total titration charge based on the time integration from the adopted base line to that calculated from the initial weight of the oxide. They are in good agreement with each other.

The base line is, as described previously, concerned with the difference of oxygen permeation rates for two cells. The oxygen permeation rate may be affected not only by temperature and oxygen fugacity but also by the voltage provided to the oxygen pump of the cell. If oxygen permeation is strongly dependent on the voltage, it is difficult to obtain an appropriate base line because the voltage provided to the sample cell changes greatly when a sample is reduced or oxidized. However, good agreement between the calculated and the observed titration charge shown in Table I reveals that oxygen permeation is not so strongly dependent on the voltage provided to the cell and the simple manner described

TABLE I

COMPARISON BETWEEN THE TITRATION CHARGE BASED ON THE TIME INTEGRAL OF A REDUCTION CURVE ($Q_{obs.}$) AND THAT FROM THE INITIAL WEIGHT OF A SAMPLE ($Q_{calc.}$)

Sample	$W_{initial}$ (mg)	$Q_{calc.}$ (coulomb)	$Q_{obs.}$ (coulomb)
NiO	30.20	78.01	78.1
$Co_{0.2}Ni_{0.8}O$	27.97	72.21	71.3
$Co_{0.4}Ni_{0.6}O$	30.97	79.90	79.6
$Co_{0.6}Ni_{0.4}O$	31.05	80.06	78.9
$Co_{0.8}Ni_{0.2}O$	31.04	79.99	77.9
CoO	25.16	64.80	64.2

previously is adequate to determine the base line, in the present experimental conditions.

It is concluded that the present method has enough accuracy for usual purpose in phase equilibrium studies. By means of the DSCT, phase relations and thermodynamic data of a multicomponent system can be obtained more easily compared with other methods such as thermogravimetry or quenching method. Now, this method is being applied to the more complicated system, Ca–V–O. Detailed appreciation for the DSCT will be clear through this work.

Acknowledgment

The author expresses his sincere thanks to Dr. K. Kato of National Institute for Research in Inorganic Materials, for his helpful suggestions throughout the present work.

References

1. H. G. Sockel and H. Schmalzried, *Ber. Bunsenges. Phys. Chem.* **72,** 745 (1968).
2. H. F. Rizzo, R. S. Gordon, and I. B. Cutler, *J. Electrochem. Soc.* **116,** 226 (1969).
3. G. B. Barbi, *J. Phys. Chem.* **68,** 2912 (1964).
4. B. E. F. Fender and F. D. Riley, *J. Phys. Chem. Solids* **30,** 793 (1969).
5. F. E. Rizzo and J. V. Smith, *J. Phys. Chem.* **72,** 485 (1968).
6. R. A. Giddings and R. S. Gordon, *J. Electrochem. Soc.* **121,** 793 (1974).
7. Y. D. Tretyakov, V. F. Komarov, N. A. Prosvirnina, and I. B. Kutsenok, *J. Solid State Chem.* **5,** 157 (1972).
8. Y. D. Tretyakov and R. A. Rapp, *Trans. AIME* **245,** 1235 (1969).
9. W. Weppner, C. Li-chuan, and W. Piekarczyk, *Z. Naturforsch. A* **35,** 381 (1980).
10. W. Weppner, C. Li-chuan, and A. Rabenau, *J. Solid State Chem.* **31,** 257 (1980).
11. T. B. Reed, "The Chemistry of Extended Defects in Non-metallic Solids" (L. Eyring and M. O'Keeffe, Eds.), p. 21, North-Holland, Amsterdam, 1970.
12. A. D. Pelton and W. T. Thompson, "Progress in Solid State Chemistry, Vol. 10" (J. O. McCaldin and G. Somorjai, Eds.), p. 119, Pergamon, New York, 1976.
13. K. Hauffe, "Treatise on Solid State Chemistry, Vol. 4" (N. B. Hannay, Ed.), p. 389. Plenum, New York, 1976.
14. G. G. Charette and S. N. Flengas, *J. Electrochem. Soc.* **115,** 796 (1968).
15. B. Björkman and E. Rósen, *Chemi. Scr.* **13,** 139 (1978–1979).
16. R. J. Moore and J. White, *J. Mater. Sci.* **9,** 1393 (1974).